Static and dynamic spin correlations in the spin-glass phase of slightly doped $La_{2-x}Sr_xCuO_4$

M. Matsuda*
RIKEN (The Institute of Physical and Chemical Research), Wako, Saitama 351-0198, Japan

M. Fujita and K. Yamada
Institute for Chemical Research, Kyoto University, Gokasho, Uji 610-0011, Japan

R. J. Birgeneau and M. A. Kastner
Department of Physics and Center for Materials Science and Engineering, Massachusetts Institute of Technology, Cambridge, Massachusetts 02139

H. Hiraka and Y. Endoh
Institute for Materials Research, Tohoku University, Katahira, Sendai 980-8577, Japan

S. Wakimoto† and G. Shirane
Department of Physics, Brookhaven National Laboratory, Upton, New York 11973
(Received 15 March 2000; revised manuscript received 28 June 2000)

Neutron-scattering experiments reveal that a diagonal spin modulation, which is a one-dimensional modulation rotated away by 45° from that in the superconducting phase, occurs universally across the insulating spin-glass phase in $La_{2-x}Sr_xCuO_4$ $(0.02 \leqslant x \leqslant 0.055)$. This establishes an intimate relation between the magnetism and the transport properties in the high-temperature copper oxide superconductors. Furthermore, it is found that the charge density per unit length estimated using a charge stripe model is almost constant throughout the phase diagram, even when the modulation rotates away by 45° at the superconducting boundary. However, at the lowest values for x the density changes approaching 1 hole/Cu as in $La_{2-x}Sr_xNiO_4$. Magnetic excitation spectra suggest that magnetic correlations change from incommensurate to commensurate at $\omega \sim 7$ meV and $T \sim 70$ K, indicating a characteristic energy for the incommensurate structure of 6–7 meV.

I. INTRODUCTION

The phase diagram of $La_{2-x}Sr_xCuO_4$ shows that the magnetic state changes dramatically with Sr doping. The parent material La_2CuO_4 exhibits three-dimensional (3D) long-range antiferromagnetic (AF) order below ~ 325 K.[1] When a small fraction of La is replaced by Sr, which corresponds to hole doping, the 3D AF order disappears and the low-temperature magnetic phase is replaced by a disordered magnetic phase in which commensurate two-dimensional (2D) short-range AF fluctuations are observed.[2,3] In crucible-grown samples the commensurate fluctuations develop a static component at low temperatures, signalling the onset of spin-glass order.

In superconducting samples, an essential feature is that the magnetic correlations become incommensurate (IC).[4–7] Detailed studies on the hole concentration dependence of the low-energy magnetic excitations have been performed by Yamada *et al.*[5] They find that the incommensurability (δ) is almost linear with hole concentration (x) with $\delta \simeq x$ below $x \sim 0.12$. Recently, static magnetic ordering has been observed in superconducting $La_{1.88}Sr_{0.12}CuO_4$ (Refs. 8 and 9) with the magnetic onset temperature near T_c. The elastic magnetic peaks are observed at the same IC positions as those of the magnetic inelastic peaks. A model that describes this behavior is that of stripe ordering of spin and charge (hole) density waves as observed in $La_{2-y-x}Nd_ySr_xCuO_4$.[10,11] In this case the charge and, concomitantly, spin stripes run approximately along the a_{tetra} or b_{tetra} axis; we label this the collinear stripe phase.

Thus the magnetism and the transport properties in the doped La_2CuO_4 system are intimately related.[12] In the insulating phase at low hole concentrations, spin-glass behavior is observed and there are strong quasielastic commensurate spin fluctuations; dynamic IC spin fluctuations persist in the superconducting phase. It has been known for some time that in $La_{2-x}Sr_xCuO_4$ the instantaneous magnetic correlations change from being commensurate to IC at the insulator-to-superconductor boundary. Recently, Wakimoto *et al.* have found that in a sample grown with the crucible-free traveling solvent floating zone technique, which results in purer crystals, the static magnetic correlations at low temperature are also IC in the insulating spin-glass $La_{1.95}Sr_{0.05}CuO_4$.[13] They have examined the intensity profiles and have shown that there are only two satellite peaks along b_{ortho},[14] while in superconducting compounds the IC peaks are located parallel to both the a_{tetra} and b_{tetra} axes. These magnetic correlations in $La_{1.95}Sr_{0.05}CuO_4$ are consistent with diagonal charge stripes, in which the stripes run along the a_{ortho} axis. Actually, such diagonal stripes have been predicted theoretically.[15–19] Diagonal stripes are also reported experimentally in insulating $La_{2-x}Sr_xNiO_4$.[20] We emphasize, however, that only a one-dimensional *spin* modulation has been observed in $La_{2-x}Sr_xCuO_4$ to-date; any associated *charge* ordering has not yet been detected. These results lead to the important conclusion that the static magnetic spin modula-

tion changes from diagonal to collinear at $x=0.055\pm0.005$, coincident with the insulator-to-superconductor transition.

A fundamental question is whether or not the diagonal one-dimensional IC magnetic correlations persist throughout the spin-glass phase down to the critical concentration of $x=0.02$ for 3D Néel ordering. The present neutron-scattering study clarifies this point and yields important information on the concentration dependence of the incommensurability. Especially, we find that at the lowest concentration within the context of the stripe model the inferred charge density is ~ 1 hole/Cu as in $La_{2-x}Sr_xNiO_4$.

Another important point is to clarify the nature of the magnetic excitations in the diagonal IC state. Intensive studies of the inelastic magnetic spectra in insulating $La_{2-x}Sr_xCuO_4$ were performed by Keimer *et al.*[3] They studied the energy and temperature dependences of the Q-integrated susceptibility. However, the Q dependence of the excitation spectra was not discussed since the detailed peak profile was not known. Matsuda *et al.* also studied the inelastic magnetic spectra in $La_{1.98}Sr_{0.02}CuO_4$,[21] in which the energy and temperature dependences of the excitation spectra were measured. They only discussed the results qualitatively since the detailed peak profile could not be clarified. Now that the static magnetic correlations have been elucidated, the excitation spectra can be analyzed qualitatively. Specifically, we found that the magnetic correlations change from being incommensurate to commensurate at $\omega\sim 7$ meV and $T\sim 70$ K, indicating a characteristic energy for the IC structure of 6–7 meV.

II. EXPERIMENTAL DETAILS

The single crystal of $La_{1.976}Sr_{0.024}CuO_4$ was grown by the traveling solvent floating zone (TSFZ) method. The crystal was annealed in an Ar atmosphere at 900 °C for 24 h. The dimensions of the rod shaped crystal were $\sim 5\Phi\times 25$ mm^3. The lattice constants were $a_{\rm ortho}=5.349$ Å, $b_{\rm ortho}=5.430$ Å ($b/a\sim 1.015$), and $c=13.151$ Å at 10 K. From the universal relation for the spin-glass transition temperature, the tetragonal-to-orthorhombic structural transition temperature, and the orthorombicity b/a,[22] the effective hole concentration was estimated to be 0.024 ± 0.003.

The neutron-scattering experiments were carried out on the cold neutron three-axis spectrometer HER and the thermal neutron three-axis spectrometer TOPAN installed at JRR-3M at the Japan Atomic Energy Research Institute (JAERI). The horizontal collimator sequences were guide-open-S-80′-80′ with the fixed incident neutron energy $E_i=5$ meV at HER and 30′-30′-S-60′-60′ with the fixed final neutron energy $E_f=14.7$ meV at TOPAN. Contamination from higher-order beams was effectively eliminated using Be filters at HER and PG filters at TOPAN. The single crystal, which was oriented in the $(HK0)_{\rm ortho}$ or $(H0L)_{\rm ortho}$ scattering plane, was mounted in a closed cycle refrigerator. In this paper, we use the low-temperature orthorhombic phase ($Bmab$) notation $(h,k,l)_{\rm ortho}$ to express Miller indices.

The crystal has a twin structure and there exist two domains. The two domains are estimated to be equally distributed from the ratio of the nuclear Bragg peak intensities from both domains. Figure 1(a) shows the scattering geometry in the $(HK0)$ scattering plane. The filled triangles correspond to the (1,0,0) and (0,1,0) Bragg points from domain A while the open triangles denote the (1,0,0) and (0,1,0) Bragg points from domain B.

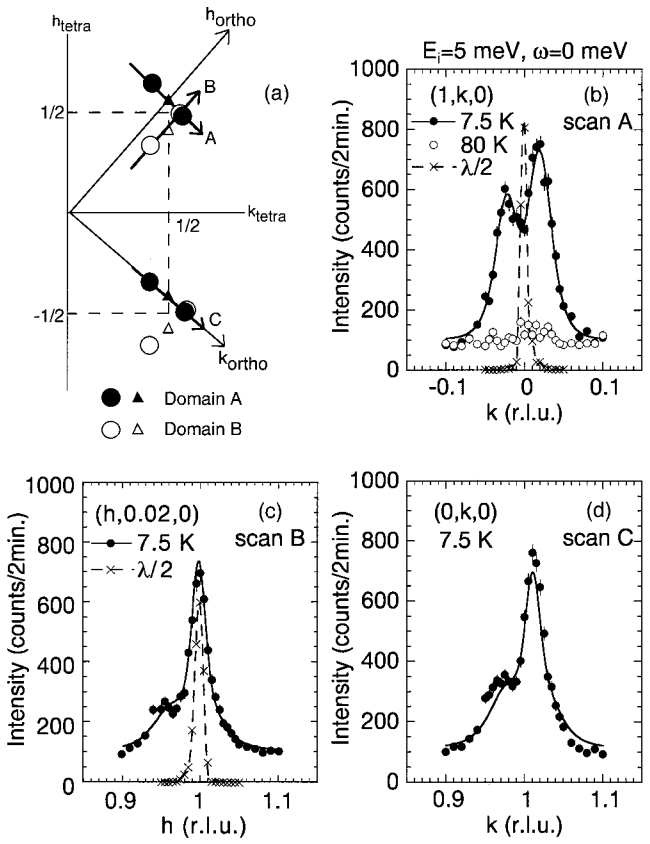

FIG. 1. (a) Diagram of the reciprocal lattice in the $(HK0)$ scattering zone. Filled and open symbols are for domains A and B, respectively. The triangles and circles correspond to nuclear and magnetic Bragg peaks, respectively. The thick arrows show scan trajectories. Transverse (b) and longitudinal elastic scans (c) and (d) around (1,0,0) and (0,1,0) at 7.5 K (filled circles) and 80 K (open circles). The crosses represent the higher-order Bragg peaks observed at (1,0,0) by removing the Be filters. The broken lines are guides to the eyes. The peak width represents the instrumental resolution. The solid lines are the results of fits to a convolution of the resolution function with 3D squared Lorentzians with $\xi_a'=94.9$ Å, $\xi_b'=39.9$ Å, $\xi_c'=3.15$ Å, and $\epsilon=0.0232$.

III. RESULTS AND DISCUSSION

A. Static properties

Below ~ 40 K elastic magnetic peaks develop and at low temperatures the peaks are clearly resolved at the IC positions $(1,\pm\epsilon,0)$ and $(0,1\pm\epsilon,0)$ with $\epsilon\sim 0.023$. This corresponds to the same diagonal one-dimensional spin modulation observed in $La_{1.95}Sr_{0.05}CuO_4$ which has $\epsilon\sim 0.064$.[13] The open and filled circles in Fig. 1(a) correspond to the IC magnetic peaks from the two domains in the $(HK0)$ zone, respectively. Figures 1(b)–1(d) show transverse and longitudinal elastic scans around (1,0,0) and (0,1,0). Two peaks are observed in the transverse scan A while one intense peak together with a weak shoulder on the low-h side is observed in the longitudinal scans B and C. The instrumental resolution at (1,0,0) can be estimated from higher-order reflections,

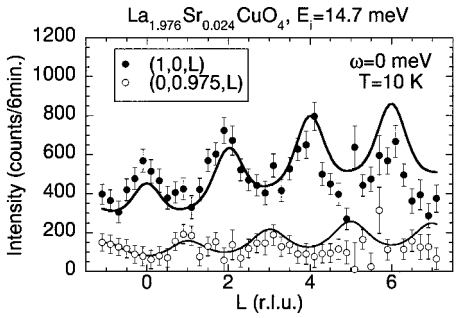

FIG. 2. Elastic scans along $(1,0,L)$ and along $(0,0.975,L)$ at 10 K. The background intensities measured at 100 K have been subtracted. The solid lines show the results of calculations with $\xi_a' = 94.9$ Å, $\xi_b' = 39.9$ Å, $\xi_c' = 3.15$ Å, and $\epsilon = 0.0232$.

which in turn are measured by removing the Be filters. As illustrated in Figs. 1(b) and (c), the magnetic peaks are much broader than the resolution along both h and k. It should be noted that, by contrast, the magnetic peaks in the superconducting state of $La_{1.88}Sr_{0.12}CuO_4$ are all resolution limited,[9] indicating that the magnetic correlation length in that system is quite large in the CuO_2 plane.

Figure 2 shows the L dependence of the magnetic elastic peaks at $(1,0,L)$ and $(0,0.975,L)$, respectively, at 10 K. The background estimated from the high-temperature data (100 K) has been subtracted so that the remaining signal is purely magnetic. These scans probe the magnetic correlations along the c axis between neighboring 2D antiferromagnetically correlated planes. Broad peaks are observed at $(1,0,even)$ and $(0,\sim 1,odd)$ which coincide with the magnetic Bragg peak positions in pure La_2CuO_4.[1] However, the magnetic intensity at $(1,0,even)$ initially increases with increasing L, implying a cluster spin-glass model as in $La_{1.98}Sr_{0.02}CuO_4$:[21] the spin system forms antiferromagnetically correlated clusters which have randomly different spin directions in the CuO_2 plane although the propagation vector of the AF order is along $a_{\rm ortho}$ in each cluster.

The solid lines in Figs. 1(b)–(d) are the results of fits to a convolution of the resolution function with 3D squared Lorentzians. The two intense peaks in Fig. 1(b) originate primarily from the magnetic signals at $(1,\pm\epsilon,0)$ in domain A while the weak shoulder in Fig. 1(c) originates from magnetic signals at $(0,1-\epsilon,\pm 1)$ in domain B. The relatively intense peaks at $(0,1\pm\epsilon,0)$ occur because of the short correlation length along the c axis, which in turn makes the $(0,1\pm\epsilon,L)$, with L odd, magnetic peaks broad along the c axis as shown in Fig. 2. The instrumental resolution function is also elongated along the c axis so that the magnetic signals are effectively integrated. The observed data are fitted with $\xi_a' = 94.9 \pm 4.0$ Å, $\xi_b' = 39.9 \pm 1.3$ Å, $\xi_c' = 3.15 \pm 0.08$ Å, and $\epsilon = 0.0232 \pm 0.0004$, where ξ_a', ξ_b', and ξ_c' represent the inverse of the half width at half maxima of the elastic peak widths in Q along the a, b, and c axes, respectively. The calculation reproduces the observed profiles quite well. The error bars represent one standard deviation statistical error limits for the assumed line shape. The true error limits, indicating possible systematic errors, are much larger. The static correlation length perpendicular to the CuO_2 plane is 3.15 Å, which is much less than the distance between nearest-neighbor CuO_2 planes ($c/2 \sim 6.5$ Å), indicating that the

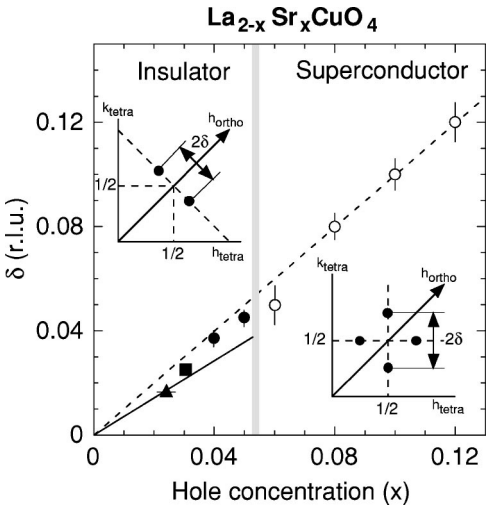

FIG. 3. Hole concentration (x) dependence of the splitting of the IC peaks (δ) in tetragonal reciprocal lattice units. Open circles indicate the data for the inelastic IC peaks reported by Yamada *et al.* (Ref. 5). Filled circles and square are the data for the elastic IC peaks reported by Wakimoto *et al.* (Refs. 14 and 29). The filled triangle is obtained from the present study. The broken and solid lines correspond to $\delta = x$ and $\epsilon = x$, respectively. The insets show the configuration of the IC peaks in the insulating phase (diagonal stripe) and the superconducting phase (collinear stripe).

static magnetic correlations are almost two dimensional. The between-plane correlation length is shorter than those in $La_{1.48}Nd_{0.4}Sr_{0.12}CuO_4$ ($\xi_c \sim 0.55c$ at 1.38 K) (Ref. 11) and $La_{1.775}Sr_{0.225}NiO_4$ ($\xi_c \sim 1.06c$ at 10 K).[20]

The solid lines in Fig. 2 show the calculated profiles using 3D squared Lorentzian profiles convoluted with the instrumental resolution function. The parameters determined above are held fixed and only the overall scale factor has been adjusted. In order to reproduce the L dependence of the $(1,0,even)$ intensity, the cluster spin-glass model,[21] as described above, has been used in the calculation. The calculation describes the observed profiles reasonably well. The slight deviation at large L in both the $(1,0,L)$ and $(0,0.975,L)$ scans probably reflects a decrease at large L of the magnetic form factor, which has been assumed to be constant in the calculation.

The diagonal magnetic stripe model thus provides a good description of the data; this is one of the most significant results of this study. The incommensurability ϵ corresponds to the inverse modulation period of the spin-density wave. Here, ϵ is defined in orthorhombic notation so that $\epsilon = \sqrt{2} \times \delta$ where δ is defined in tetragonal units. As shown in Fig. 3, δ follows the linear relation $\delta = x$ reasonably well over the range $0.03 \leqslant x \leqslant 0.12$ which spans the insulator-superconductor transition. In a charge stripe model this corresponds to a constant charge per unit length in both the diagonal and collinear stripe phases, or equivalently, 0.7 and 0.5 holes per Cu, respectively, because of the $\sqrt{2}$ difference in Cu spacings in the diagonal and collinear geometries. Our value for $x = 0.024$ definitely deviates from the $\delta = x$ line and instead appears to be close to ~ 1 hole/Cu as in $La_{2-x}Sr_xNiO_4$ where there is ~ 1 hole/Ni (Ref. 20) along the diagonal stripes. This suggests that as the hole concentration is decreased, in the context of the stripe model, the hole

TABLE I. Hole concentration dependence of the static spin correlation length in $La_{2-x}Sr_xCuO_4$. A blank means that the peak width is too broad to determine ξ_c'. It is noted that ξ_b' in the $x=0.02$ sample is obtained on the assumption that the magnetic correlations are commensurate. This value could become larger (~ 45 Å) if the magnetic correlations are incommensurate with $\epsilon = x$.

x	ξ_a' (Å)	ξ_b' (Å)	ξ_c' (Å)
0.02[a]	160	25	4.7
0.024[b]	94.9±4.0	39.9±1.3	3.15±0.08
0.05[c]	25	33	

[a]Reference 21.
[b]This work.
[c]Reference 14.

concentration evolves progressively from ~ 0.5 hole/Cu at $x=0.12$ to 1 hole/Cu at $x=0.024$. This behavior is very different from that in $La_{2-x}Sr_xNiO_4$, where the hole density is ~ 1 hole/Ni over a wide range of hole concentrations in the insulating phase albeit at rather larger hole densities.[23] We note that Machida and Ichioka predict 1 hole/Cu throughout the diagonal stripe phase.[24]

The static spin correlation lengths, which are derived from the inverse peak widths in Q, in $La_{2-x}Sr_xCuO_4$ ($x=0.02$, 0.024, and 0.05) are summarized in Table I. With increasing hole concentration, the peak widths both parallel and perpendicular to the CuO_2 plane rapidly broaden. In $La_{1.95}Sr_{0.05}CuO_4$, an L scan shows that the peak width along L is much broader than that in $La_{1.976}Sr_{0.024}CuO_4$, indicating that the magnetic correlations are more two dimensional.[14]

There are at least two possible origins of the finite correlation lengths in the CuO_2 plane for the static order in the spin-glass $La_{2-x}Sr_xCuO_4$. The first is that the lengths simply measure the spin decoherence distance of the AF spin clusters. The second is that the disorder originates primarily from a random distribution of stripe spacings and orientations as discussed by Tranquada *et al.*[25] It is noted that a rotation of the stripe orientation away from the a_{tetra} and b_{tetra} axes is observed in La_2CuO_{4+y} (Ref. 26) and $La_{1.88}Sr_{0.12}CuO_4$ (Ref. 27). Further experiments and theoretical calculations will be required to choose between these possibilities.

B. Magnetic excitations

As mentioned in the previous section, static magnetic correlations in the spin-glass phase has been revealed. We now consider how the inelastic magnetic correlations behave in the spin-glass phase of $La_{2-x}Sr_xCuO_4$. Neutron inelastic scattering measurements were performed in $La_{1.976}Sr_{0.024}CuO_4$. The measurements were performed in the $(H0L)$ scattering plane. We first carried out the measurements in the $(HK0)$ scattering plane, in which the elastic IC magnetic peaks can be resolved reasonably well since the instrumental resolution is narrower than the intrinsic peak widths as shown in Fig. 4(a). However, with increasing transfer energy, the resolution becomes worse and the magnetic intensity decreases due to the structure factor. Because of these two effects, it is very difficult to follow the energy dependence of the excitation spectra. In the $(H0L)$ scattering

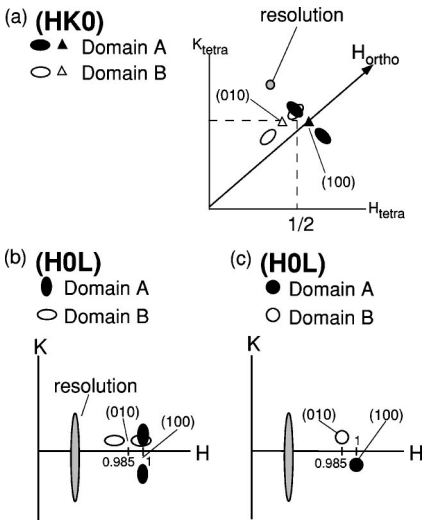

FIG. 4. The schematic configuration of the magnetic peaks in the $(HK0)$ and $(H0L)$ scattering planes. The instrumental resolution is elongated perpendicular to the scattering plane. The ellipsoids and circles represent magnetic peaks. (a) and (b) show scattering configurations in the IC phase. As shown in the text, the IC magnetic peaks are anisotropic. In the commensurate phase (c), the peaks are considered to be isotropic.

plane, since the resolution is elongated perpendicular to H, as shown in Fig. 4(b), the IC peak cannot be well resolved. However, as we will show later, the intrinsic peak configuration can be estimated by fitting to model functions. The advantage of the measurements in the $(H0L)$ scattering plane is that the measurements can be performed with increased scattering intensity.

First, we performed constant-Q scans around (π,π) in order to study the magnetic anisotropy in $La_{1.976}Sr_{0.024}CuO_4$.

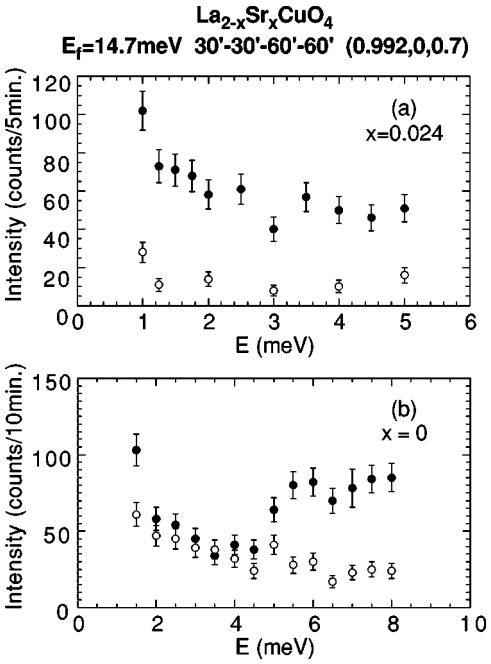

FIG. 5. Filled circles show constant-Q scans at (0.992,0,0.7) measured at $T=10$ K in $La_{1.976}Sr_{0.024}CuO_4$ (a) and in La_2CuO_4 (b). Open circles show background intensities measured at (1.15,0,0.7).

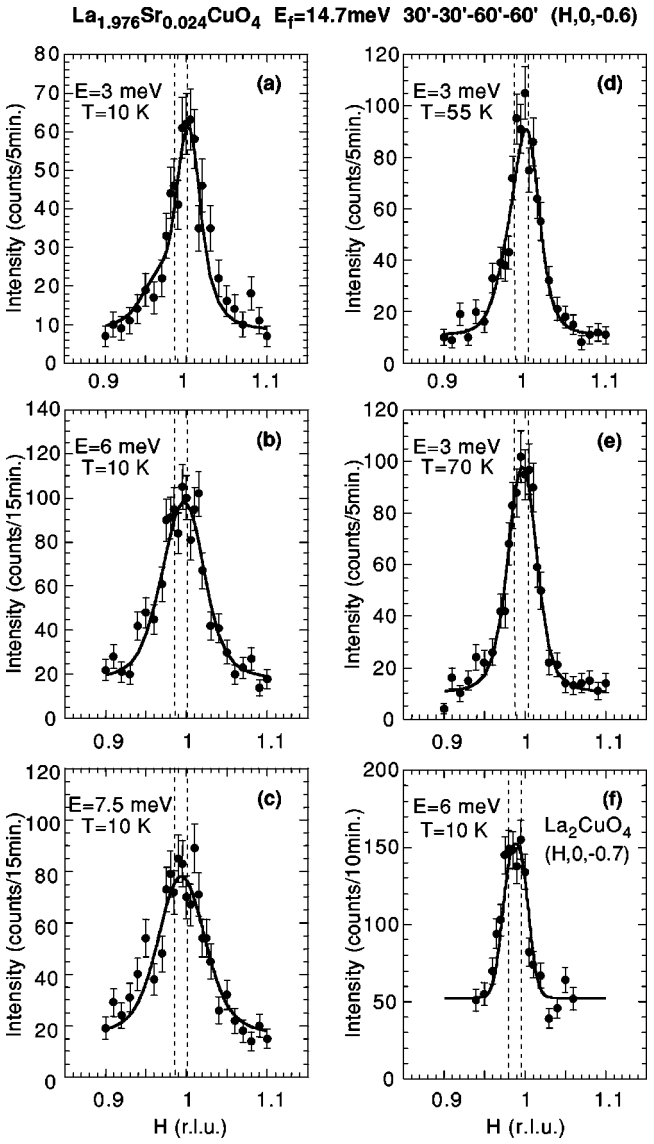

FIG. 6. Neutron inelastic scans along $(H,0,-0.6)$ and $(H,0,-0.7)$ at various energies and temperatures in $La_{1.976}Sr_{0.024}CuO_4$ and in La_2CuO_4. The solid lines are the results of fits to a convolution of the resolution function with 3D squared Lorentzians. The broken lines show the centers of the peaks $(1,0,L)$ and $(0,1,L)$ determined from the nuclear Bragg peak positions.

Figure 5(a) shows the result of constant-Q scans at (0.992,0,0.7), which corresponds to just the midpoint between (1,0,0.7) and (0,1,0.7). The background intensities are measured at (1.15,0,0.7). The magnetic intensity decreases gradually with increasing energy, indicating that the magnetic excitation spectrum is gapless in $La_{1.976}Sr_{0.024}CuO_4$. For comparison, constant-Q scans in pure La_2CuO_4 with the same spectrometer condition are shown in Fig. 5(b). An excitation gap due to the out-of-plane anisotropy is found at ~ 5 meV, which is consistent with that observed previously.[28]

Figure 6 shows constant-ω scans in the $(H0L)$ scattering plane at various energies and temperatures. A sharp excitation peak is centered at $H=1$ at $\omega=3$ meV and $T=10$ K. On the other hand, the peak position shifts progressively to lower H at higher energies and temperatures.

We speculate that this behavior may be explained as follows. At 3 meV, the magnetic peaks exist at IC positions as observed in the elastic scans in the $(HK0)$ scattering zone as shown in Fig. 4(a). Since the instrumental resolution elongated vertically integrates the magnetic signal around $H=1$ very effectively in the $(H0L)$ scattering plane, as shown in Fig. 4(b), a sharp and intense peak centered at $H=1$ is observed while a weak tail is found at lower H. The solid line in the Fig. 6(a) is the result of a calculation assuming that the magnetic peaks are located at exactly the same positions as those determined from the elastic measurements in the $(HK0)$ scattering plane. As excitation energy is increased, the peak separation appears to to become smaller. The excitation spectrum at 6 meV is fitted to 3D Lorentzians. The fitting parameters are the peak separation ϵ, the isotropic inverse inelastic peak width in the CuO_2 plane ξ''_{ab}, and the amplitude. The inverse inelastic peak width along the c axis ξ''_c is fixed at 3.15 Å, which is the same as ξ'_c. The solid line in the Fig. 6(b) is the result of a fit to the 3D Lorentzians with $\epsilon=0.0096\pm0.0068$ and $\xi''_{ab}=48\pm12$ Å. Finally, the magnetic correlations appears to become commensurate and isotropic at 9 meV as shown in Fig. 4(c). In this case, there exist two equi-intense peaks at $(0,1,-0.6)$ $(H=0.985)$ and $(1,0,-0.6)$ $(H=1)$ resulting in one broad peak located at $H\sim0.99$. The solid line in Fig. 6(c) is the result of a fit to the 3D Lorentzians with $\xi''_c=3.15$ Å (fixed) and $\xi''_{ab}=42\pm13$ Å. ϵ is fixed at 0 since it becomes very close to 0 even when fitted. From these results, we conclude that magnetic correlations change from being incommensurate to commensurate between ~6 and ~7.5 meV.

The commensurate magnetic correlations at higher energies are similar to those observed in pure La_2CuO_4 above the gap energy ~5 meV as shown above. The excitation spectrum in pure La_2CuO_4 at 6 meV is shown in Fig. 6(f). The spectrum is consistent with the peak configuration as shown in Fig. 4(c) since the magnetic correlations are commensurate and isotropic. The peak width is resolution limited, indicating that the correlation length is very long in the CuO_2 plane. This is in striking contrast to the situation in $La_{1.976}Sr_{0.024}CuO_4$. The solid line in Fig. 6(f) is the result of a calculation assuming the 3D Lorentzians with $\xi''_{ab}=700$ Å (fixed), $\xi''_c=1$ Å (fixed), and $\epsilon=0$ (fixed).

The temperature dependence of the excitation spectra in $La_{1.976}Sr_{0.024}CuO_4$ is quite similar to the energy dependence. A sharp excitation peak centered at $H=1$ at low temperatures shifts to lower H with increasing temperature. The solid line in the Fig. 6(d) is the result of a fit to an assumed 3D Lorentzian line shape with $\epsilon=0.0113\pm0.0068$ and $\xi''_{ab}=60\pm11$ Å. ξ''_c is fixed at 1 Å since the system becomes magnetically 2D above ~40 K. ϵ and ξ''_{ab} do not change sensitively with changes in ξ''_c in the fitting. The solid line in Fig. 6(e) is the result of a fit to a 3D Lorentzian with $\xi''_{ab}=62\pm10$ Å and $\xi''_c=1$ Å (fixed). ϵ is fixed at 0 since it becomes very close to 0 even when fitted. From these results, we conclude that the magnetic correlations change from being incommensurate to commensurate between 55 and 70 K.

Figure 7 represents a summary of the neutron inelastic measurements in $La_{1.976}Sr_{0.024}CuO_4$. The open and filled

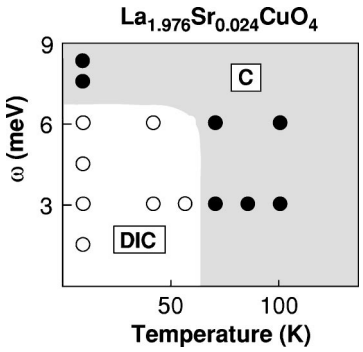

FIG. 7. Energy-temperature phase diagram in $La_{1.976}Sr_{0.024}CuO_4$. Open and filed circles represent that the magnetic correlations are diagonal incommensurate (DIC) and commensurate (C), respectively.

circles signify that the magnetic correlations are diagonal IC and commensurate, respectively. The diagonal IC phase exists below $\omega \sim 7$ meV and $T \sim 70$ K (~ 6 meV). This result indicates that the characteristic energy for the diagonal IC structure is 6–7 meV.

IV. SUMMARY

In brief, we find that a short-range static one-dimensional diagonal spin modulation exists at low temperatures across the entire insulating spin-glass region in $La_{2-x}Sr_xCuO_4$. Further, within the context of a spin and charge stripe model the charge density per unit length is almost constant for all values of x, but shows a significant deviation near the spin-glass 3D Néel boundary suggesting stability of diagonal stripes with 1 hole/Cu at low x.

The magnetic excitation spectra suggest that magnetic correlations change from diagonal incommensurate to commensurate at $\omega \sim 7$ meV and $T \sim 70$ K. Above these energy and temperature the magnetic correlations are similar to those in pure La_2CuO_4 although the range of order in the CuO_2 plane is much shorter in $La_{1.976}Sr_{0.024}CuO_4$.

ACKNOWLEDGMENTS

We would like to thank A. Aharony, K. Katsumata, and K. Machida for stimulating discussions. This study was supported in part by the U.S.-Japan Cooperative Program on Neutron Scattering, by a Grant-in-Aid for Scientific Research from the Japanese Ministry of Education, Science, Sports and Culture, by a Grant for the Promotion of Science from the Science and Technology Agency, and by CREST. Work at Brookhaven National Laboratory was carried out under Contract No. DE-AC02-98CH10886, Division of Material Science, U.S. Department of Energy. The research at MIT was supported by the National Science Foundation under Grant No. DMR97-04532 and by the MRSEC Program of the National Science Foundation under Award No. DMR98-08941.

*Present address: Advanced Science Research Center, Japan Atomic Energy Research Institute, Tokai, Ibaraki 319-1195, Japan.

†Also at Department of Physics, Massachusetts Institute of Technology, Cambridge, Massachusetts 02139.

[1] D. Vaknin, S. K. Sinha, D. E. Moncton, D. C. Johnston, J. Newsam, C. R. Safinya, and H. King, Phys. Rev. Lett. **58**, 2802 (1987).

[2] B. J. Sternlieb, G. M. Luke, Y. J. Uemura, T. M. Riseman, J. H. Brewer, P. M. Gehring, K. Yamada, Y. Hidaka, T. Murakami, T. R. Thurston, and R. J. Birgeneau, Phys. Rev. B **41**, 8866 (1990).

[3] B. Keimer, N. Belk, R. J. Birgeneau, A. Cassanho, C. Y. Chen, M. Greven, M. A. Kastner, A. Aharony, Y. Endoh, R. W. Erwin, and G. Shirane, Phys. Rev. B **46**, 14 034 (1992).

[4] S.-W. Cheong, G. Aeppli, T. E. Mason, H. A. Mook, S. M. Hayden, P. C. Canfield, Z. Fisk, K. N. Clausen, and J. L. Martinez, Phys. Rev. Lett. **67**, 1791 (1991).

[5] K. Yamada, C. H. Lee, K. Kurahashi, J. Wada, S. Wakimoto, S. Ueki, H. Kimura, Y. Endoh, S. Hosoya, G. Shirane, R. J. Birgeneau, M. Greven, M. A. Kastner, and Y. J. Kim, Phys. Rev. B **57**, 6165 (1998).

[6] H. Yoshizawa, S. Mitsuda, H. Kitazawa, and H. Katsumata, J. Phys. Soc. Jpn. **57**, 3686 (1988).

[7] R. J. Birgeneau, Y. Endoh, K. Kakurai, Y. Hidaka, T. Murakami, M. A. Kastner, T. R. Thurston, G. Shirane, and K. Yamada, Phys. Rev. B **39**, 2868 (1989).

[8] T. Suzuki, T. Goto, K. Chiba, T. Shinoda, T. Fukase, H. Kimura, K. Yamada, M. Ohashi, and Y. Yamaguchi, Phys. Rev. B **57**, R3229 (1998).

[9] H. Kimura, K. Hirota, H. Matsushita, K. Yamada, Y. Endoh, S.-H. Lee, C. F. Majkrzak, R. Erwin, G. Shirane, M. Greven, Y. S. Lee, M. A. Kastner, and R. J. Birgeneau, Phys. Rev. B **59**, 6517 (1999).

[10] J. M. Tranquada, B. J. Sternlieb, J. D. Axe, Y. Nakamura, and S. Uchida, Nature (London) **375**, 561 (1995).

[11] J. M. Tranquada, J. D. Axe, N. Ichikawa, Y. Nakamura, S. Uchida, and B. Nachumi, Phys. Rev. B **54**, 7489 (1996).

[12] M. A. Kastner, R. J. Birgeneau, G. Shirane, and Y. Endoh, Rev. Mod. Phys. **70**, 897 (1998).

[13] S. Wakimoto, G. Shirane, Y. Endoh, K. Hirota, S. Ueki, K. Yamada, R. J. Birgeneau, M. A. Kastner, Y. S. Lee, P. M. Gehring, and H. S. Lee, Phys. Rev. B **60**, R769 (1999).

[14] S. Wakimoto, R. J. Birgeneau, M. A. Kastner, Y. S. Lee, R. Erwin, P. M. Gehring, S. H. Lee, M. Fujita, K. Yamada, Y. Endoh, K. Hirota, and G. Shirane, Phys. Rev. B **61**, 3699 (2000).

[15] K. Machida, Physica C **158**, 192 (1989).

[16] M. Kato, K. Machida, H. Nakanishi, and M. Fujita, J. Phys. Soc. Jpn. **59**, 1047 (1990).

[17] D. Poilblanc and T. M. Rice, Phys. Rev. B **39**, 9749 (1989).

[18] H. Schulz, J. Phys. (Paris) **50**, 2833 (1989).

[19] J. Zaanen and O. Gunnarsson, Phys. Rev. B **40**, 391 (1990).

[20] J. M. Tranquada, D. J. Buttrey, and V. Sachan, Phys. Rev. B **54**, 12 318 (1996).

[21] M. Matsuda, Y. S. Lee, M. Greven, M. A. Kastner, R. J. Birgeneau, K. Yamada, Y. Endoh, P. Böni, S.-H. Lee, S. Wakimoto, and G. Shirane, Phys. Rev. B **61**, 4326 (2000).

[22] M. Fujita and K. Yamada (unpublished).

[23] H. Yoshizawa, T. Kakeshita, R. Kajimoto, T. Tanabe, T. Katsufuji, and Y. Tokura, Phys. Rev. B **61**, R854 (2000).

[24] K. Machida and M. Ichioka, J. Phys. Soc. Jpn. **68**, 2168 (1999).

[25] J. M. Tranquada, N. Ichikawa, and S. Uchida, Phys. Rev. B **59**, 14 712 (1999).

[26] Y. S. Lee, R. J. Birgeneau, M. A. Kastner, Y. Endoh, S. Wakimoto, K. Yamada, R. W. Erwin, S.-H. Lee, and G. Shirane, Phys. Rev. B **60**, 3643 (1999).
[27] H. Kimura, H. Matsushita, K. Hirota, Y. Endoh, K. Yamada, G. Shirane, Y. S. Lee, M. A. Kastner, and R. J. Birgeneau, Phys. Rev. B **61**, 14 366 (2000).
[28] B. Keimer, R. J. Birgeneau, A. Cassanho, Y. Endoh, M. Greven, M. A. Kastner, and G. Shirane, Z. Phys. B: Condens. Matter **91**, 373 (1993).
[29] S. Wakimoto and S.-H. Lee (private communication).